Impact of traffic flows and wind directions on air pollution concentrations in Seoul, Korea

Article *in* Atmospheric Environment · May 2011

DOI: 10.1016/j.atmosenv.2011.02.050

2 authors, including:

Jean-Michel Guldmann
The Ohio State University
157 PUBLICATIONS **862** CITATIONS

Pre-Publication Manuscript

Atmospheric Environment
2011, Vol. 45, pp. 2803-2810

IMPACT OF TRAFFIC FLOWS AND WIND DIRECTIONS ON AIR POLLUTION CONCENTRATIONS IN SEOUL, KOREA

Youngkook Kim

The Korea Transport Institute
Goyang-si, Gyeonggi-do, 411-701
Korea
youngkim@koti.re.kr

Jean-Michel Guldmann

Department of City and Regional Planning
The Ohio State University
Columbus, OH 43210, USA
guldmann.1@osu.edu

Abstract
Vehicle emissions are responsible for a substantial share of urban air pollution concentrations. Various integrated air quality modeling systems have been developed to analyze the consequences of air pollution caused by traffic flows. However, the quantitative relationship between vehicle-kilometers-traveled (VKT) and pollution concentrations while considering wind direction effects has rarely been explored in the context of land-use regression models (LUR). In this research, VKTs occurring within circular buffers around air pollution monitoring stations are simulated, using a traffic assignment model, and weighted by eight wind directions frequencies. The relationships between monitored pollution concentrations and weighted VKTs are estimated using regression analysis. In general, the wind-direction-weighted VKT variable increases the explanatory power of the models, particularly for nitrogen dioxide and carbon monoxide. The case of ozone is more complex, due to the effects of solar radiation, which appears to overwhelm the effects of wind direction in the afternoon hours. The statistical significance of the weighted VKT variable is high, which makes the models appropriate for impact analysis of traffic flow growth.

Keywords
Vehicle-kilometers-traveled; Wind direction; Pollution concentration; Regression modeling

1. Introduction

Despite improvements in vehicle emission control technology, the recent rapid growth in vehicle ownership and average trip length has created unhealthy air quality in urban areas. Transportation is known to be responsible for a substantial share of urban air pollution emissions, such as carbon monoxide (CO), nitrogen dioxide (NO_2), and volatile organic compounds (VOC), and indirectly so for ozone (O_3) concentrations. It is reasonable to expect that, as vehicle-kilometers-traveled (VKT) increase, ambient air pollution concentrations also increase. Several studies have uncovered meaningful relationships between vehicle emissions and air pollution concentrations (Roorda-Knape et al., 1999; Potoglou and Kanaroglou, 2005; Kim and Guldmann, 2007; Lau et al., 2008). In addition, Kim (2010) has found a significant relationship between hourly seasonal average pollution concentration and VKT. Pollutants emitted by motor vehicles impact the spatial and temporal distribution of ambient concentrations, which are also determined by meteorological factors, such as wind direction (WD) (Faiz, 1993; Small and Kazimi, 1995; McHugh et al., 1997; Lau et al., 2008).

Integrated modeling systems for air quality management have been developed in several countries, including AirGIS in Denmark (Jensen et al., 2001), Air Quality Information System in Norway (Bøhler et al., 2002), and Traffic Emission Modelling and Mapping Suite in England (Namdeo et al., 2002). However, the quantitative relationship between pollution concentrations and traffic volumes, while accounting for WD impacts, has rarely been investigated. Air movements are key determinants of pollution concentrations because horizontal and vertical airflows influence the mixing and transport of air pollutants. The former represent wind and the latter turbulence (Seaman, 2000). Land use regression (LUR) modeling has been recently conducted to establish relationships between monitored pollution concentrations at Air Quality Monitoring (AQM) stations and the surrounding physical environment (Jerrett et al., 2007). Hoek et al. (2008) critically review recent LUR studies, with land-use and transport-related variables as predictors. In general, transport variables, such as traffic counts, road length, and inverse distance to highway, have strong positive relationships with pollutant concentrations.

The emission source of cyclohexane near a heavy industrial region in Houston, Texas, is correctly identified using nonparametric regression applied to hourly concentrations and WD (Henry, Chang, and Spiegelman, 2002). However, despite the impact of WD on pollution concentrations, as demonstrated in the use of atmospheric diffusion models, wind variables are rarely included in LUR models. One exception is Arain et al. (2007), who include wind effects in their LUR models, using wind field data interpolated from observed WD data. They calculate whether the monitoring point is located up- or down-wind from highway emission sources, and the inclusion of wind variables enhances the performance of their models. In this research, hourly VKTs around AQM stations are estimated and weighted by eight wind direction frequencies, and the relationships between monitored pollution concentrations and these WD-weighted VKTs are examined.

2. Research method and data collection

2.1 Overview

To assess the relationship between pollution concentrations and WD-weighted VKT (WVKT), three data sets are required: (1) hourly air pollution concentrations, (2) traffic assignment over the transportation network, using a typical day origin/destination (OD) matrix, and (3) hourly monitored WD frequencies and traffic counts. Eleven circular buffer are delineated around each AQM, with a radius varying from 500 to 5,500 meters. Using a Geographic Information System (GIS), these buffers are overlaid onto the transportation network and VKT is calculated for each

link within any circular buffer[1]. Using available hourly traffic counts data, the estimated daily VKT is divided into hourly VKTs. Regression models are then estimated for five pollution concentrations (NO_2, SO_2, CO, PM10: particles with diameter $\leq$10μm, and O_3) as dependent variables, and hourly VKT as the explanatory variable. To account for the WD effect, the circular buffer zone is subdivided into eight sectors, each sector is overlaid onto the transportation network, and VKT for each sector is computed and weighted by WD frequency.

2.2 Air pollution data

Hourly air pollution concentrations are routinely measured at 34 AQMs in Seoul, Korea, and have been downloadable from the website of the National Institute of Environmental Research of Korea (NIER, 2010)[2] for the year 2003. These AQMs are distributed over the Seoul metropolitan area, as illustrated in Figure 1, with 27 AQMs classified as urban background ones, that monitor average air quality and assess whether standards are attained. The other 7 AQMs are located near crowded traffic roads to measure roadside air quality. Pollution concentrations are measured in ppb (parts per billion) units for NO_2, CO, O_3, and SO_2. In the case of PM10, the unit is $\mu g/m^3$ (microgram per cubic meter). Pollutant sampling tools are set up at a height of around 2.5 meters above ground level at each road. In contrast, urban background AQMs are located away from major roadways, on the roofs of two- or three-story public buildings, such as elementary schools and public offices. One-hour average concentrations are calculated based on measurements every five minutes (12 readings per hour) (Korea Ministry of Environment, 2005).

Different methods are used to measure pollution concentrations: the chemiluminescent method for NO_2, the non-dispersive infrared method for CO, the ultraviolet (UV) photometric method for O_3, the pulse UV fluorescence method for SO_2, and the β-ray absorption method for PM10. In order to mitigate the effects of power outages, uninterrupted power suppliers are installed in the AQMs to secure continuous measurements of pollution concentrations. Each month, monitoring instruments are regularly inspected. Monitored pollution data are screened twice. The first screening is performed in the regional air quality management offices, where instrument and outliers are routinely checked. Except for obvious instrumental errors, these data are then transmitted to the National Ambient air Monitoring Information System (NAMIS), managed by NIER. If the monitored concentrations are significantly different from those of the previous month and/or from those of the same month of the previous year, or if they exceed environmental standards, NIER investigates the reasons for these unusual concentrations, including nearby pollution sources, fuel consumptions, traffic flows, and meteorological factors, and then reports the results. Only valid data is published, and the conditions of validity are different depending on the time intervals. An hourly average data is considered valid only if there are more than 9 five-minute measurements. In the case of daily average data, the number of valid hourly data must be more than 18. A valid monthly average data is calculated based on more than 540 hourly data. A valid annual average data requires more than 6,570 hourly data (Korea Ministry of Environment, 2010). In this research, the hourly-averaged pollution concentrations of NO_2, SO_2, CO, PM10, and O_3 are used to assess their relationships with VKT and WD-weighted VKT.

[1] During geo-processing, a transportation link which crosses a buffer boundary is divided into two or several split links depending on its length. Because geo-processing does not change attribute data, split links have the same attribute data, in this case, the same VKT. To correct the attribute data for split links, it is necessary to calculate the lengths of the original and split links and then apportion VKT to each split link based on link lengths.

[2] http://www.nier.go.kr/

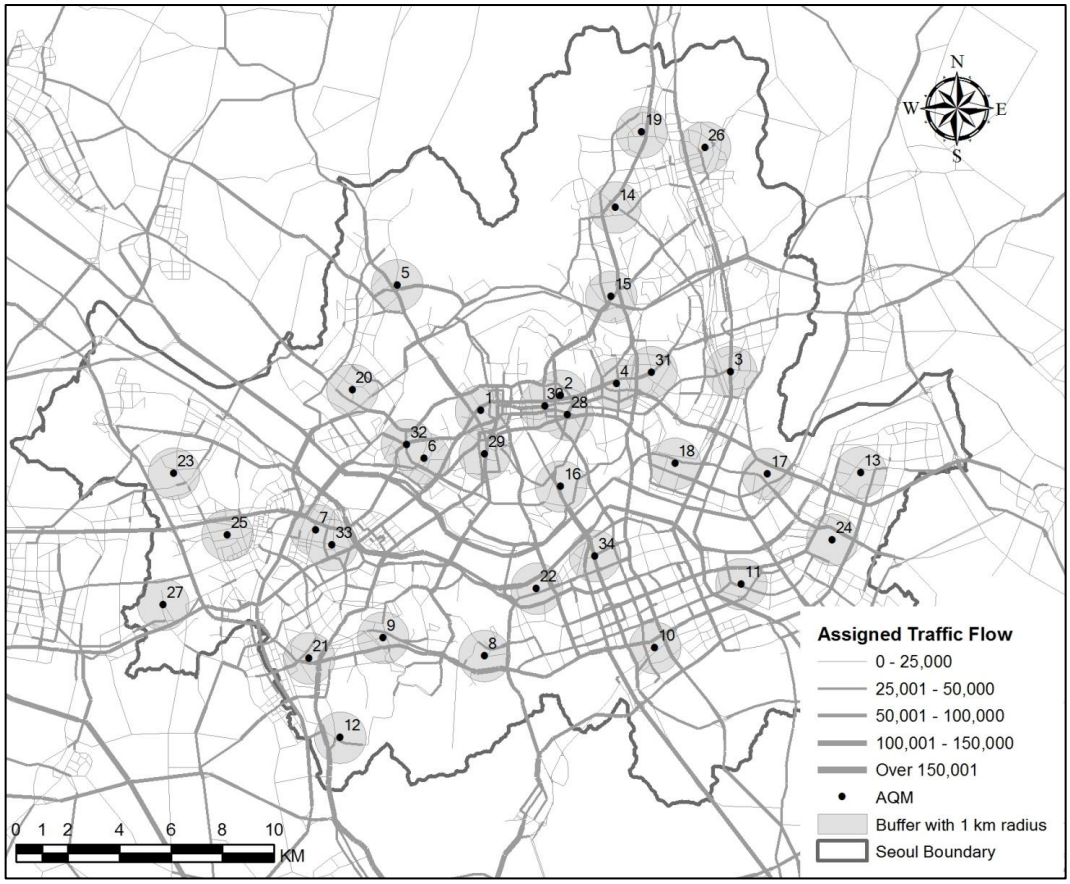

Figure 1 Location of AQMs and assigned traffic flows in Seoul, Korea

2.3 Traffic assignment and VKT calculation

The Seoul Development Institute (SDI) has released a typical day OD matrix and transportation network data for the Capital region of Korea, which includes the Seoul, Incheon, and Gyeonggi provinces (SDI, 2007)[3]. These OD and network data are used in a traffic assignment model, TransCAD®, which allows for six assignment methods: all-or-nothing, capacity restraint, incremental, stochastic, system optimum, and user equilibrium (UE). In order to choose the appropriate method, 56 road links are selected to compare monitored traffic flows and assigned flows under the 6 methods. The UE method is selected, and VKT is then calculated by multiplying link length and assigned traffic volume for each link (Kim, 2010).

To measure the impacts of traffic emissions on air pollution concentrations, VKTs are summed up over circular buffers around each AQM, using GIS functions, such as buffering, intersecting, and database calculations. The distances between traffic emissions and receptors are important in determining the concentrations at receptors. Therefore, several circular buffers with radii of 500 to 5,500 meters are delineated around each AQM. The VKTs on the transportation links within the circular buffers are estimated as follows: (1) the buffers are overlaid onto the traffic network; (2) the attributes of the intersected links are calculated using ArcGIS® and Python® scripts; (3) the traffic flows estimated with the traffic assignment model are allocated to the intersected links.

Since the AQM concentrations are measured hourly, the assigned traffic flows are disaggregated on an hourly basis, using monitored traffic counts data collected over a week at 4

[3] http://sdihard.webhard.co.kr

different road categories: cordon line (39 locations), Han river bridges (18 locations), arterial roads (34 locations), and central business districts roads (26 locations). These counts were supervised by the Seoul Metropolitan Police Agency (SMPA) and are reported on the Seoul city government website (Seoul City Government, 2010)[4] and in the 2003 Seoul Traffic Survey Report (SMPA, 2004).

2.4 Wind direction and WVKT calculation

To account for WD impacts on pollution concentrations, eight-sector[5] wind directions are considered for each AQM and the estimated VKTs for each buffer are also sub-divided into these eight sectors. Hourly WD data have been downloaded from the Korea Meteorological Administration (2008) website. The annual frequencies for the eight WD sectors, as computed with these hourly observations, are illustrated in Figure 2. The prevailing WDs in Seoul are from the West and the North-East.

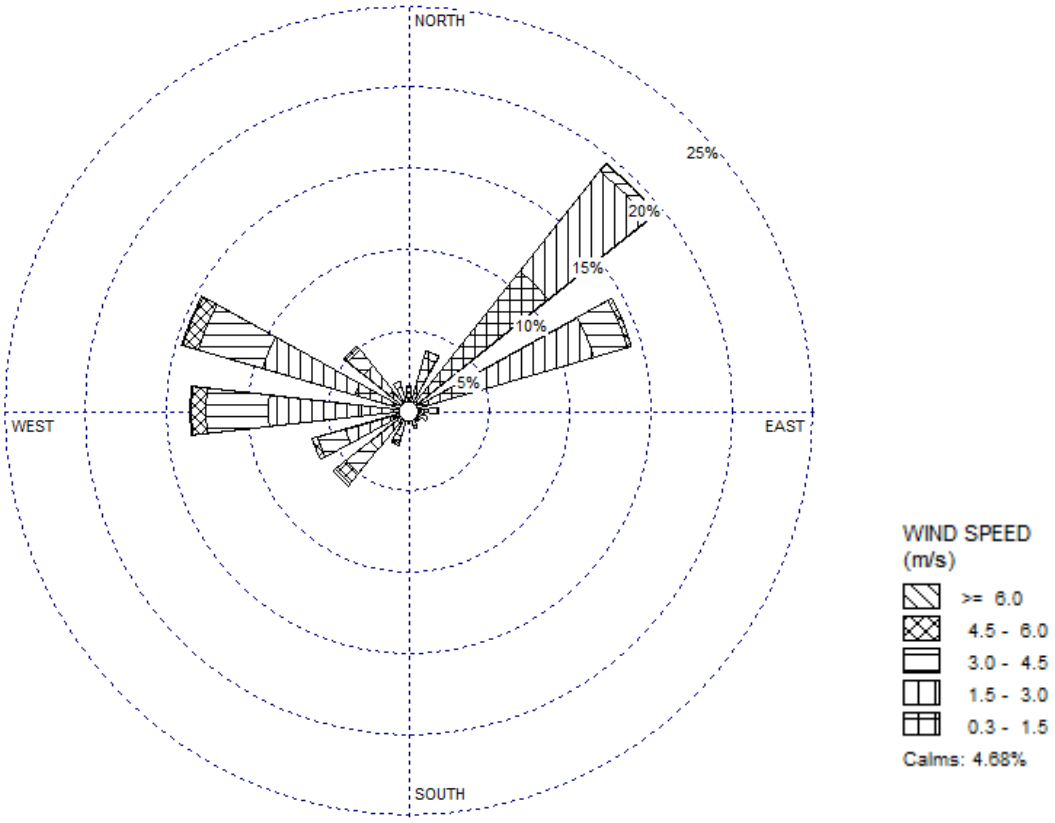

Figure 2 Annual wind rose for Seoul, Korea

Since pollutants are primarily dispersed downwind from sources, WD affects pollution concentrations. In order to calculate WVKT, the WD-weighted VKT, the frequencies of the eight-sector wind directions and calm conditions are used for weighting the VKTs of each AQM. The following indices are defined:

h: Hour of day $(1 \rightarrow 24)$,

[4] http://stat.seoul.go.kr/index.jsp

[5] Eight-sector includes N-NNE, NE-ENE, E-ESE, SE-SSE, S-SSW, SW-WSW, W-WNW, and NW-NNW.

t: Day of year ($1 \rightarrow 365$),
d: Wind direction ($1 \rightarrow 8$),
i: AQM ($1 \rightarrow 34$),
R: Buffer radius ($500 \rightarrow 5500$m).

Let VKT_{diRht} be the sum of all VKTs in sector d of buffer R around AQM i at hour h of day t in 2003. Wind directions and calm conditions are defined, for each hour and day, by the following binary numbers: WD_{dht} and $CALM_{ht}$. If wind speed is less than 0.2 meters/sec, then $CALM_{ht} = 1$ and all $WD_{dht} = 0$. If the wind speed is greater than 0.2 meters/sec and the direction is d, then $WD_{th} = 1$ for direction d and zero for all the other directions, and the calm index is also set to zero. Wind direction is measured every five minutes and the dominant direction is recorded as the hourly wind direction. Thus, the retained direction is not necessarily the only one during the hour. Figure 3 presents an eight-sector, 1,500-meter radius buffer around AQM No. 10.

The final variable, $WVKT_{iRh}$, represents the average value of WVKT for hour h over the 365 days of the year, summed up over all eight sectors. It is computed as follows:

$$WVKT_{iRh} = [\sum_{t=1\rightarrow 365} (\sum_{d=1\rightarrow 8} WD_{dht} . VKT_{diRht}) + CALM_{ht} . (\sum_{d=1\rightarrow 8} VKT_{diRht})]/365 \qquad (1)$$

3. Traffic flows and pollution concentrations patterns

A qualitative exploratory analysis of concentrations and traffic patterns is a necessary input to the development of quantitative regression models (Section 4). Figures 4-8 display the average hourly traffic flows and concentrations for NO_2, SO_2, CO, PM10, and O_3. The hourly roadside and background concentrations are averages over the 7 roadside and 27 background AQMs, respectively.

The traffic flow displays a typical urban pattern characterized by two peaks, in the morning and the evening. Traffic emissions are the major source of directly emitted pollutants in urban regions (Jo and Park, 2005; Carslaw and Beevers, 2004a; Fujita et al. 2003). As shown in Figures 4-7, the hourly patterns of pollutants concentrations for both roadside and background AQMs are similar, with a steep increase in the morning, starting at 6 AM when morning traffic increases, a trough at midday, and an evening peak. As expected, the roadside AQM concentrations are higher than the background ones, except for ozone (Pandey et al., 2008). Direct pollutant emissions from motor vehicles (NO_2, SO_2, CO, PM10) appear to be closely correlated with traffic flows on Figures 4-7. [6]. However, this is not the case for O_3 on Figure 8.

Tropospheric O_3 is produced by photochemical reactions involving VOCs and nitrogen oxides (NO_x) emitted by both anthropogenic activities and biological processes. However, counterintuitively, several studies report that heavily traveled roadside areas are less polluted by O_3 than urban background regions (Jo and Park, 2005; Kim, 2007; Kim, 2010). Figure 8 points to roadside O_3 concentrations lower than the background ones, particularly in the afternoon, in line with past results.

[6] According to Derwent and Hertel (1998), over 90% of nitrogen compounds are emitted in the form of nitric oxide (NO). Only less than 10% of nitrogen is directly emitted NO_2 form. NO produced in the combustion process, however, mainly reacts with O_3 and other radicals in the ambient atmosphere within a few seconds after its emission, and is transformed into NO_2. Thus, strictly, NO_2 can be classified as a secondary product, but, because of its quick and complete reaction, NO_2 can be regarded as direct emission from vehicles.

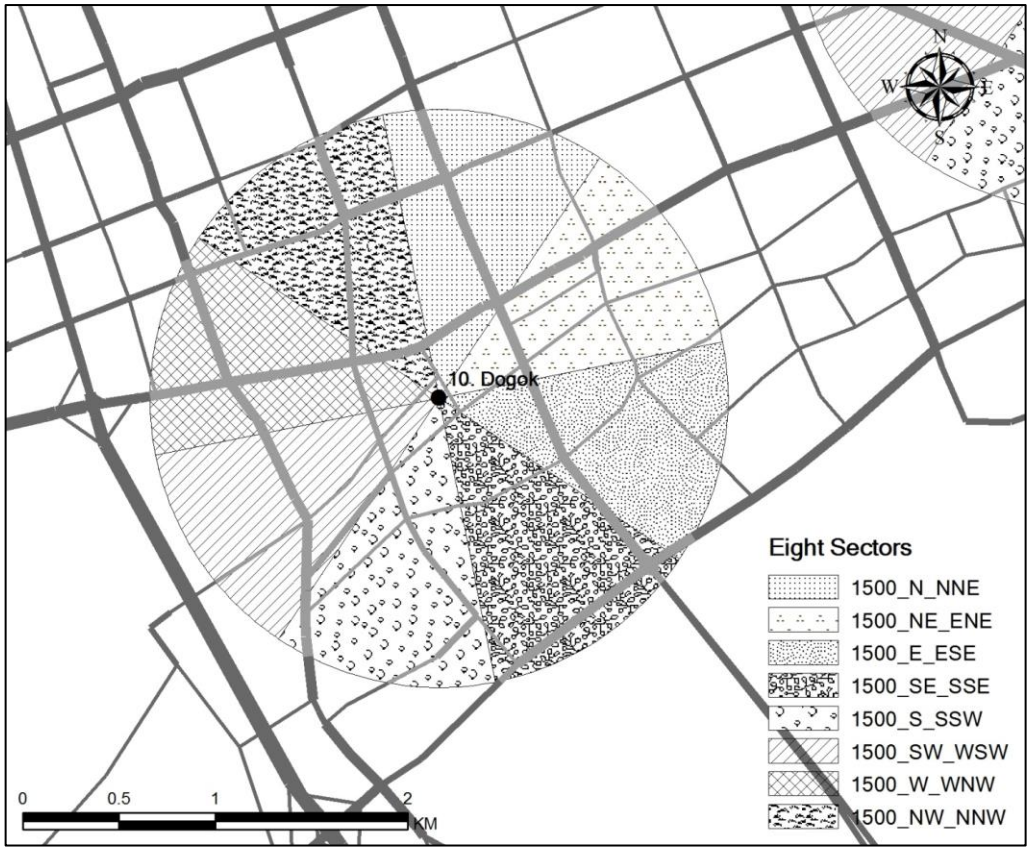

Figure 3 Eight-sector buffer around AQM No. 10 with a 1,500 meter radius

The formation rates of tropospheric O_3 are determined by both the ratio and amounts of precursor chemicals and the intensity of solar radiation. The presence of ultraviolet (UV) radiation (hv) is an essential factor, because the photolysis of NO_2 is initiated by UV (Eq. 2). The tropospheric O_3 is generated by combining ground-state atomic oxygen, O, with an oxygen molecule, O_2, in the presence of a third body M that absorbs excessive energy and stabilizes the formed O_3 molecule (Eq. 3).

$$NO_2 + hv \rightarrow NO + O \quad (2)$$

$$O + O_2 + M \rightarrow O_3 + M \quad (3)$$

As seen in Figure 8, O_3 concentrations display increase steeply when solar radiation starts. Usually the peak of UV radiation occurs around 1 PM, but the highest O_3 concentrations occur around 4 PM. Mid-afternoon high-temperature and clear sky are the best conditions to produce O_3 (Derwent and Hertel, 1998). Since O_3 is a secondary product generated by a series of chemical reactions (Eqs. 2 and 3) and destroyed by O_3 titration (Eq. 4), the accumuluation of O_3 depends upon these creation and destruction rates.

$$NO + O_3 \rightarrow NO_2 + O_2 \quad (4)$$

As long as the creation rate is higher than the destruction one, O_3 concentration increases. This may be a possible reason for the time lag between peak UV and peak O_3 concentration. After

the 4 PM ozone peak, the concentration of O_3 decreases, because the creation of O_3 is constrained by decreased UV radiation in the late afternoon. In the evening, O_3 is no longer being formed and thus remains at steady levels during the night. Freshly emitted NO increases along with the increase of morning traffic flows, scavenging the ambient O_3 and, as a result, the lowest concentration occurs around 7 ~ 8 AM. From a spatial viewpoint, the destruction of O_3 (Eq. 4) can be more easily observed at roadside areas than at urban background ones, because freshly emitted NO from motor vehicles is more abundant at roadside areas, and one can therefore expect that higher VKTs lead to lower O_3 concentrations.

There are two notable phenomena observed in the hourly pattern of NO_2 concentrations (Figure 4). One is that the depth of the trough is shallow in the roadside pattern, as compared to the background one. The reason may be that, during daytime, UV ray stimulates the photolysis of NO_2, but freshly emitted NO from the tail pipe is abundant near the roadside, which alleviates the effects of photolysis. The other is that the peak concentration occurs during the evening at both roadside and background AQMs. These highest evening NO_2 concentrations can be explained as follows: (1) the accumulated O_3 during daytime and NO emissions in the evening traffic peak facilitate O_3 titration, leading to high NO_2 creation rates; (2) NO_2 photolysis no longer takes place after sunset.

Since diesel vehicles are the major source of SO_2 emission in Korea's urban regions, SO_2 concentrations are observed to be higher near roadside areas. Due to the difference between gasoline and diesel prices in Korea, the number of diesel vehicles has increased in recent years, resulting in a 34.6% share of vehicle registrations in 2003 (Korea Ministry of Environment, 2005). However, while this share is rising, the contribution of motor vehicles to SO_2 concentrations is smaller than their contributions to other pollutants, such as NO_2 and CO. According to the US EPA (2000), transportation-related emission contributes around 5% of total SO_2 emission. In the Seoul Metropolitan area, this contribution was 11% in 2003.

4. Wind direction impacts and pollution concentrations regression models

The previous exploratory analysis suggests two regression modeling approaches: 1) pooling all hourly data across all AQMs in the cases of NO_2, SO_2, CO, and PM10, and (2) pooling these data across all AQMs for each hour separately in the case of O3. The first approach is based on the apparent close correlations between concentrations and traffic flows, whereas the second approach accounts for the variations of the impact of traffic across the hours of the day, due to the effects of solar radiation. Define C_{ih} as the average hourly concentration of a given pollutant at AQM i during hour h, and VKT_{iRh} as the average VKT value around AQM i during hour h (no account for WD). The regression models estimated with VKT and WVKT are then:

$$C_{ih} = \alpha_{1R} + \beta_{1R}\, VKT_{iRh} \qquad (5)$$

$$C_{ih} = \alpha_{2R} + \beta_{2R}\, WVKT_{iRh} \qquad (6)$$

The impacts of accounting for wind directions can be assessed by comparing the R^2 of the estimated Eqs. (5) and (6). The regression results are presented in Table 1 for NO_2 and SO_2, and in Table 2 for CO and PM10. Each regression model is estimated with 816 (34 AQMs × 24 hrs) observati

Table 1 NO_2 and SO_2 regression results for different buffers

	Buffer Radius (meters)	Vehicle Kilometers Traveled (VKT)			Wind Direction Weighted Vehicle Kilometers Traveled (WVKT)		
		Parameter	t Value	R^2	Parameter	t Value	R^2
NO_2	500	1118.40	11.71***	0.14	6460.49	10.22***	0.11
	1000	410.09	15.41***	0.23	3089.95	16.82***	0.26
	1500	235.52	17.94***	0.28	1875.06	20.61***	0.34
	2000	141.73	17.81***	0.28	1157.81	21.37***	0.36
	2500	99.32	18.30***	0.29	789.11	21.43***	0.36
	3000	73.19	18.78***	0.30	591.54	22.70***	0.39
	3500	55.84	19.21***	0.31	457.70	23.31***	0.40
	4000	43.58	19.28***	0.31	357.29	23.43***	0.40
	4500	34.98	19.34***	0.31	289.58	23.34***	0.40
	5000	28.71	19.00***	0.31	235.72	22.49***	0.38
	5500	24.18	19.04***	0.31	197.96	22.32***	0.38
SO_2	500	202.54	13.98***	0.19	1243.25	13.03***	0.17
	1000	59.32	13.97***	0.19	451.74	15.40***	0.23
	1500	33.53	15.82***	0.24	244.65	15.99***	0.24
	2000	19.99	15.52***	0.23	137.92	14.66***	0.21
	2500	13.66	15.42***	0.23	94.81	14.85***	0.21
	3000	9.82	15.28***	0.22	72.18	15.87***	0.24
	3500	7.14	14.67***	0.21	52.80	15.07***	0.22
	4000	5.57	14.70***	0.21	41.67	15.34***	0.22
	4500	4.44	14.58***	0.21	33.78	15.30***	0.22
	5000	3.55	13.91***	0.19	27.01	14.54***	0.21
	5500	2.93	13.58***	0.18	22.16	14.03***	0.19

*: <0.1, **:<0.05, ***:<0.01

Table 2. CO and PM10 regression results for different buffers

	Buffer Radius (meters)	Vehicle Kilometers Traveled (VKT)			Wind Direction Weighted Vehicle Kilometers Traveled (WVKT)		
		Parameter	t Value	R^2	Parameter	t Value	R^2
CO	500	213.96	7.91***	0.07	1632.47	9.41***	0.10
	1000	64.78	8.19***	0.08	657.08	12.34***	0.16
	1500	34.46	8.52***	0.08	350.10	12.52***	0.16
	2000	15.91	6.39***	0.05	169.53	9.73***	0.10
	2500	11.34	6.64***	0.05	127.02	10.84***	0.13
	3000	7.69	6.20***	0.05	95.59	11.36***	0.14
	3500	5.94	6.38***	0.05	74.83	11.73***	0.14
	4000	4.49	6.20***	0.05	56.38	11.29***	0.14
	4500	3.60	6.20***	0.05	44.52	10.93***	0.13
	5000	2.87	5.92***	0.04	35.21	10.31***	0.12
	5500	2.45	6.02***	0.04	29.06	10.06***	0.11
PM10	500	482.91	4.60***	0.03	5610.07	8.45***	0.08
	1000	71.82	2.31**	0.01	988.76	4.55***	0.02
	1500	33.21	2.08**	0.01	418.98	3.65***	0.02
	2000	8.57	0.89	0.00	151.20	2.17**	0.01
	2500	5.72	0.86	0.00	102.47	2.16**	0.01
	3000	2.07	0.43	0.00	61.79	1.80*	0.00
	3500	3.35	0.93	0.00	58.47	2.24*	0.01
	4000	4.05	1.44	0.00	53.69	2.65***	0.01
	4500	4.01	1.78*	0.00	47.10	2.86***	0.01
	5000	3.20	1.71*	0.00	39.12	2.86***	0.01
	5500	2.29	1.46	0.00	30.55	2.64***	0.01

*: <0.1, **:<0.05, ***:<0.01

As expected, using the variable WVKT to account for WD impacts provides, in most cases, better regression results than when using VKT. The R^2 averaged over the 11 buffers increases from (1) 0.28 to 0.34 for NO_2, (2) 0.209 to 0.214 for SO_2, (3) 0.055 to 0.134 for CO, and (4) 0.002 to

0.017 for PM10. The most significant increases are for NO_2 (6%) and CO (8%). There is very little change in the case of SO_2, and the PM10 model has a low explanatory power with either variable. The explanatory power of the model varies with the size of the buffer. In the case of NO_2, the R^2 regularly increases with the buffer radius, reaching its maximum (0.40) around 4 km when using WVKT. On the other hand, WVKT for buffer radii less than 1.5 km provides the largest R^2 for SO_2, CO, and PM10.

The regression coefficients β_{1R} and β_{2R} are statistically significant at the 1% level for the NO_2, SO_2, and CO models, with either VKT or WVKT. In the case of PM10 and WVKT, 7 models are significant at the 1% level, and the others at least at the 10% level. However, the PM10 models with VKT are only significant for radii up to 1,500 meters. The generally high significance of the explanatory variables suggests that the models would be useful for impact analysis, that is, predicting the increase in concentrations resulting from a given increase in traffic flow ($\Delta C = \beta.\Delta WVKT$). However, except perhaps in the NO_2 case, these models cannot be used for predicting concentrations because of their low R^2 and large error terms representing the unobserved variables.

CO is produced by the incomplete combustion of carbon-containing materials. Since motor vehicles are its major source in urban areas, traffic flows have a significant positive impact on CO concentrations. Using WVKT almost double the explanatory power of the model, as compared to using VKT. However the maximum R^2 is 0.16, significantly lower than in the NO_2 case. One possible reason is that the molecular weight of CO is less than that of air, and hot CO freshly emitted from tailpipes tends to be buoyant. This may accelerate the vertical rather than the horizontal dispersion of CO.

The sources of PM vary widely, from human activities to natural sources, including dusts from roads, construction sites, and agricultural land, combustion of fossil fuels (electric generation and internal combustion engines), ammonia from agriculture, marine aerosols, pollen, biomass burning, wind blowing from China (yellow sand), and secondary particles, such as ammonium sulfate and ammonium nitrate. A source of fine PM emissions in urban regions is diesel vehicles. With advances in catalytic converter technology, gasoline vehicles with converters emit far less PM than diesel vehicles. Therefore, directly emitted elemental carbon soot from diesel vehicles, re-suspended dust from roads, and secondary acidic particles are major contributors of PM at urban roadside areas. According to Zhu et al. (2002), the concentration of ultra fine particles (diameter $\leq$ 0.1μm) decreases by 60 to 80% within 100 meters downwind from a road. Therefore, in the PM10 case, the 500-meter buffer provides the best explanation, which is still a low R^2=0.08. This suggests that the model does not account for important unobserved effects, such as non-traffic related sources of PM10. It may also be that the share of diesel vehicles in the traffic flow varies across the network. As a consequence, VKT or WVKT would not be good proxies for diesel PM10 emissions.

Diesel vehicles are responsible for SO_2 emissions. However, the small share of diesel vehicles in the overall vehicle fleet, a possibly variable share of these vehicles across the network, and the existence of other important sources of SO_2 (fuel combustion for heating, manufacturing, and electricity production), are all possible reasons for why accounting for WD fails to improve the SO_2 models.

In the case of O_3, the following models are estimated for each hour separately:

$$C_{ih} = \alpha_{1Rh} + \beta_{1Rh}\, VKT_{iRh} \qquad (7)$$

$$C_{ih} = \alpha_{2Rh} + \beta_{2Rh}\, WVKT_{iRh} \qquad (8)$$

Each hourly model is estimated with 34 observations. A buffer with a 4.5 km radius is found to provide the best results, which are presented in Table 3.

Table 3 O_3 hourly regression results for a buffer radius of 4,500 meters

Time	Vehicle Kilometers Traveled (VKT)			Wind Direction Weighted Vehicle Kilometers Traveled (WVKT)		
	Parameter	t Value	R^2	Parameter	t Value	R^2
00-01	-13.64	-2.64**	0.18	-64.62	-3.00***	0.22
01-02	-17.33	-2.34**	0.15	-82.41	-2.69**	0.19
02-03	-22.75	-2.31**	0.14	-110.21	-2.50**	0.16
03-04	-25.07	-1.97*	0.11	-139.79	-2.11**	0.12
04-05	-22.29	-1.69	0.08	-115.28	-1.82*	0.09
05-06	-16.92	-1.78*	0.09	-84.44	-1.87*	0.10
06-07	-7.94	-2.00*	0.11	-41.32	-2.12**	0.12
07-08	-3.98	-1.80*	0.09	-28.39	-2.09**	0.12
08-09	-4.46	-2.09**	0.12	-27.43	-2.39**	0.15
09-10	-9.08	-3.38***	0.26	-55.34	-3.54***	0.28
10-11	-14.19	-4.02***	0.34	-103.24	-4.15***	0.35
11-12	-19.55	-4.18***	0.35	-133.73	-4.16***	0.35
12-13	-25.19	-3.86***	0.32	-180.35	-3.73***	0.30
13-14	-27.79	-3.80***	0.31	-196.59	-3.65***	0.29
14-15	-30.03	-3.91***	0.32	-219.53	-3.72***	0.30
15-16	-31.41	-4.04***	0.34	-213.13	-3.93***	0.33
16-17	-30.75	-4.34***	0.37	-210.80	-4.18***	0.35
17-18	-26.83	-4.69***	0.41	-191.98	-4.27***	0.36
18-19	-21.10	-4.98***	0.44	-145.54	-4.94***	0.43
19-20	-17.89	-5.08***	0.45	-117.24	-5.51***	0.49
20-21	-15.79	-4.87***	0.43	-114.16	-5.71***	0.50
21-22	-12.92	-4.44***	0.38	-74.78	-5.22***	0.46
22-23	-11.85	-3.64***	0.29	-71.12	-4.31***	0.37
23-24	-11.55	-3.20***	0.24	-63.71	-3.73***	0.30

During any given hour, under assumed steady-state meteorological conditions, O_3 concentrations are determined by the rates of O_3 creation and destruction. Table 3 shows that all the hourly coefficients are negative, which implies that O_3 concentrations decrease with increasing traffic (VKT) across the Seoul Metropolitan region. If NO_x-saturated conditions are prevalent, as is the case of Seoul, an increase in VKT induces more O_3 titration, and consequently leads to lower O_3 concentrations. NO freshly emitted from motor vehicles reacts with nearby O_3, decreasing O_3 concentrations. Accounting for WD impacts on VKT increases the explanatory power of the models, but from 11 AM to 7 PM. Except for these 8 hours, the average R^2 increases from 0.21 with VKT to 0.25 with WVKT. Since solar radiation accumulation peaks around 3-4 PM, O_3 is intensely created in the afternoon, and this effect probably overwhelms the possible effects of WD in explaining O_3 concentrations, hence the lack of model improvement from noon to late afternoon.

5. Conclusion

The relationships between the average hourly concentrations of five air pollutants (NO_2, O_3, SO_2, CO, and PM10) and the average hourly VKTs in circular buffers around AQMs have been investigated. Hourly VKTs are positively related the concentrations of the directly emitted pollutants: NO_2, SO_2, CO, and PM10. In contrast, hourly O_3 concentrations are negatively related to VKT, pointing to O_3 destruction (titration) due to increasing emissions of nitrogen oxide. Using WD-weighted VKTs increases the explanatory powers of the models in most cases, but particularly

so for NO_2 and CO. In the case of O_3, however, using WVKTs does not enhance model power during the afternoon hours.

References

Arain, M. A., Blair, R., Finkelstein, N., Brook, J. R., Sahsuvaroglu, T., Beckerman, B., Zhang, L., Jerrett M. (2007). The use of wind fields in a land use regression model to predict air pollution concentrations for health exposure studies. *Atmospheric Environment, 41*(16), 3453-3464.

Bøhler, T., K. Karatzas, G. Peinel, T. Rose, and R. San Jose (2002). Providing multi-modal access to environmental data–customizable information services for disseminating urban air quality information in APNEE. *Computers, Environment and Urban Systems* 26, pp. 39-61.

Carslaw, D. C., and Beevers, S. D. (2004). Investigating the potential importance of primary NO_2 emissions in a street canyon. *Atmospheric Environment, 38*(22), 3585-3594.

Derwent, R.G. and O. Hertel (1998). "Transformation of Air Pollutants" in J. Fenger, O. Hertel, and F. Palmgren(eds.) *Urban Air Pollution-European Aspects*. Dordrecht, Netherlands: Kluwer Academic Publishers, pp. 137-160.

Faiz, A. (1993). Automotive emissions in developing countries—relative implications for global warming, acidification and urban air quality. *Transportation Research* A 27, pp. 167–186.

Fujita, E. M., Stockwell, W. R., Campbell, D. E., Keislar, R. E., and Lawson, D. R. (2003). Evolution of the magnitude and spatial extent of the weekend ozone effect in California's south coast air basin, 1981-2000. *Journal of the Air & Waste Management Association, 53*, 802-815.

Henry, R. C., Chang, Y., and Spiegelman, C. H. (2002). Locating nearby sources of air pollution by nonparametric regression of atmospheric concentrations on wind direction. *Atmospheric Environment, 36*(13), 2237-2244.

Hoek, G., Beelen, R., de Hoogh, K., Vienneau, D., Gulliver, J., Fischer, P., et al. (2008). A review of land-use regression models to assess spatial variation of outdoor air pollution. *Atmospheric Environment, 42*(33), 7561-7578.

Jensen, S.S., R. Berkowicz, H.S. Hansen, and O. Hertel (2001). A Danish decision-support GIS tool for management of urban air quality and human exposures. *Transportation Research Part D.* Vol. 6, pp. 229-241.

Jerrett, M., Arain, M. A., Kanaroglou, P., Beckerman, B., Crouse, D., Gilbert, N. L., Brook, J.R., Finkelstein, N., Finkelstein, M.M. (2007). Modeling the intraurban variability of ambient traffic pollution in Toronto, Canada. *Journal of Toxicology & Environmental Health: Part A, 70*(3), 200-212.

Jo, W.K. and J.H. Park (2005). Characteristics of roadside air pollution in Korean metropolitan city (Daegu) over last 5 to 6 years: temporal variations, standard exceedances, and dependence on meteorological conditions. *Chemosphere* 59, pp. 1557–1573.

Kim, Y. (2007). Air pollution concentration, urban traffic flow and vegetation area: Focus on cities in Gyeonggi province. *Gyeonggi Research Institute Paper Competition*, Gyeonggi-do, South Korea. 2-33 (Korean version).

Kim, Y. (2010). *Impacts of transportation, land uses, and meteorology on urban air quality*. Ph.D. Dissertation, Ohio State University, Columbus, Ohio, USA.

Kim, Y. and J.M. Guldmann (2007). Urban Air Pollution, Traffic Volume, and Road Congestion, Presented at 48th Annual Meeting of the Association of Collegiate Schools of Planning, Milwaukee, WI, October 2007.

Korea Meteorological Administration (2008). Meteorological data application website, http://minwon.kma.go.kr/index.jsp, Accessed May 30, 2010.

Korea Ministry of Environment (2005). *2005 Environment White Paper.* Seoul, Korea.

Korea Ministry of Environment (2010). *Installation and operation guidelines for air quality monitoring stations.* Seoul, Korea.

Lau, J., W.T. Hung, C.S. Cheung, and D. Yuen (2008). Contributions of roadside vehicle emissions to general air quality in Hong Kong. *Transportation Research Part D* 13, pp. 19–26.

McHugh, C.A, D.J. Carruthers, and H.A. Edmunds (1997). ADMS-Urban: an air quality management system for traffic, domestic and industrial pollution. *International Journal of Environment and Pollution*, Vol. 8, Nos. 3-6, pp. 666-674.

Namdeo, A., G. Mitchell, and R. Dixon (2002). TEMMS: An integrated package for modelling and mapping urban traffic emissions and air quality. *Environmental Modelling and Software* 17, pp. 179-190.

NIER (2010). Request for data disclosure. http://www.nier.go.kr/, Accessed March 10, 2010

Pandey, S.K., K-H. Kim, S-Y. Chung, S-J. Cho, M-Y. Kim, and Z-H Shon (2008). Long-term study of NOx behavior at urban roadside and background locations in Seoul, Korea. *Atmospheric Environment* 42, pp. 607-622.

Potoglou, D. and P.S. Kanaroglou (2005). Carbon monoxide emissions from passenger vehicles: predictive mapping with an application to Hamilton, Canada. *Transportation Research Part D* 10, pp. 97-109.

Roorda-Knape, M.C., N.A.H. Janssen, J. de Hartog, P.H.N. Von Vliet, H. Harssema, and B. Brunekreef (1999). Traffic related air pollution in city districts near motorways. *The Science of the Total Environment* 235, pp. 339-341.

SDI (2007). Future traffic demand data in Seoul. http://sdihard.webhard.co.kr, Accessed January 5, 2007.

Seaman, N. L. (2000). Meteorological modeling for air-quality assessments. *Atmospheric Environment*, *34*(12-14), 2231-2259.

Seoul City Government (2010). Traffic counts data http://www.seoul.go.kr/info/organ/subhomepage/transport/traffic_data/statisitcs/traffic/traffic1/11166_index.html, Accessed May 5, 2010

SMPA (2004). *2003 Seoul Traffic Survey Report*, Seoul, Korea.

Small, K.A. and C. Kazimi (1995). On the cost of air pollution from motor vehicles, *Journal of Transport Economics and Policy* 29, pp. 7-32.

US EPA. (2000). *National air pollutant emission trends, 1900-1998* (EPA-454/R-00-002 ed.). Research Triangle Park, NC: Office of Air Quality Planning and Standards.

Zhu, Y., W.C. Hinds, S. Kim, S. Shen, and C. Sioutas (2002). Study of ultrafine particles near a major highway with heavy-duty diesel traffic, *Atmospheric Environment* 36, pp. 4323-4335.